

$E1 - E2$ interference in the Coulomb dissociation of ${}^8\text{B}$

P. Banerjee and R. Shyam

*Theory Group, Saha Institute of Nuclear Physics,
1/AF Bidhan Nagar, Calcutta - 700 064, INDIA*

(January 14, 2022)

We investigate the effects arising out of the $E1 - E2$ interference in the Coulomb dissociation of ${}^8\text{B}$ at beam energies below and around 50 MeV/nucleon. The theory has been formulated within a first order semiclassical scheme of Coulomb excitation, in which both the ground state and the continuum state wave functions of ${}^8\text{B}$ enter as inputs. We find that the magnitude of the interference could be large in some cases. However, there are some specific observables which are free from the effects of the $E1 - E2$ interference, which is independent of the models used to describe the structure of ${}^8\text{B}$. This will be useful for the analysis of the breakup data in relation to the extraction of the astrophysical factor $S_{17}(0)$.

PACS numbers: 25.60.-t, 25.70.De, 25.40.Lw

I. INTRODUCTION

The Coulomb dissociation (CD) method provides an alternate indirect way to determine the cross sections for the radiative capture reaction ${}^7\text{Be}(p, \gamma){}^8\text{B}$ at low relative energies [1], which is a key reaction of the $p-p$ chain through which energy is generated in the sun. The rate of this reaction is the most uncertain nuclear input to the standard solar model calculations [2], which affects the high energy solar neutrino flux and bears significantly on the solar neutrino problem. The CD method reverses the radiative capture by the dissociation of a projectile (the fused system) in the Coulomb field of a target, by making the assumption that nuclei do not interact strongly and the electromagnetic excitation process is dominated by a single multipolarity [1]. Therefore, one has to pin down a kinematical domain where breakup cross sections due to different multiplicities ($E1$ and $E2$) can be clearly separated from each other. At the same time, it is also necessary to investigate the importance of the $E1 - E2$ interference effects which has not been considered so far in most of the analyses of the Coulomb dissociation data of ${}^8\text{B}$.

The magnitudes of the $E1 - E2$ interference cross sections could be appreciable for certain observables in the Coulomb dissociation of ${}^8\text{B}$. It was shown in Refs. [3,21] that the dissociation of ${}^8\text{B}$ around 45 MeV/nucleon beam energy is dominated by $E1$ transitions but the interference with $E2$ amplitudes produces large asymmetries in the angular and momentum distributions of the breakup fragments. This fact has been used in a recent measurement of the parallel momentum distribution of the ${}^7\text{Be}$ fragment resulting from the breakup of ${}^8\text{B}$ on a Pb target at 44 MeV/nucleon beam energy to put constraint on the contributions of the $E2$ component in the breakup of ${}^8\text{B}$ [5].

In this paper, our aim is to investigate the role of the $E1 - E2$ interference effects in the analysis of the Coulomb dissociation data at beam energies 25.8 MeV at

Notre Dame [6] and around 50 MeV/nucleon measured at RIKEN [7,8]. We would like to examine the importance of the interference effects in different cases and try to see whether they could be really absent in the above data. To this end, we have developed a first order semiclassical theory for the electromagnetic excitation of a composite nucleus leading to continuum final states which allows to estimate the $E1$ and $E2$ breakup contributions separately as well as their interference. Our formulation is different from that of Refs. [3,21] in the sense that we do not assume straight line trajectories for the motion of the projectile in the Coulomb field of the target nucleus. Our theory is closer to that of Baur and Weber [9] where triple differential cross sections with respect to the relative and centre of mass (c.m.) angles and energies of the fragments are determined. However, we have used a more general coupling scheme of angular momenta and spins than those in Ref. [9].

We organize the paper as follows. The theoretical formalism has been described in section 2. We describe the structure model adopted for ${}^8\text{B}$ in section 3. The results and discussions on them are presented in section 4. Finally, the summary and conclusions are given in section 5.

II. FORMALISM

We consider the following reaction

$$a + A \rightarrow c + v + A, \quad (1)$$

in which the composite projectile $a(= c + v)$ breaks up into a core c and a valence particle v in the Coulomb field of the target nucleus A which remains in the ground state (elastic breakup). We consider electric transitions of dipole and quadrupole types only. It is to be noted that the $M1$ transition contribution is small for the reactions considered here at beam energies < 52 MeV/nucleon [10].

In the initial channel, for given spins s_{c_i} and s_{v_i} of the core and valence particles, the projectile wave function is

$$\psi_{I_i M_i}(\vec{r}) = \sum_{l_i L_i} \left[[Y_{l_i}(\hat{r}) \otimes \chi_{s_{v_i}}]_{L_i} \otimes \chi_{s_{c_i}} \right]_{I_i M_i} \times \frac{f_{(L_i s_{c_i}) I_i}(r)}{r}. \quad (2)$$

In the above, l_i is the orbital angular momentum of the valence particle relative to the core and I_i is the total spin of the projectile in its ground state with projection M_i . χ 's are the spin wave functions of the core and the valence particle.

More explicitly

$$\begin{aligned} \psi_{I_i M_i}(\vec{r}) = & \left[\sum_{\substack{l_i m_{l_i} \\ L_i M_{L_i} \\ m_{v_i} m_{c_i}}} (-1)^{l_i + s_{v_i} - M_{L_i}} \sqrt{2L_i + 1} \right. \\ & \times \begin{pmatrix} l_i & s_{v_i} & L_i \\ m_{l_i} & m_{v_i} & -M_{L_i} \end{pmatrix} Y_{l_i m_{l_i}}(\hat{r}) \chi_{s_{v_i} m_{v_i}} \left. \right] \\ & \times (-1)^{L_i + s_{c_i} - M_i} \sqrt{2I_i + 1} \begin{pmatrix} L_i & s_{c_i} & I_i \\ M_{L_i} & m_{c_i} & -M_i \end{pmatrix} \\ & \times \chi_{s_{c_i} m_{c_i}} \frac{1}{r} f_{(L_i s_{c_i}) I_i}(r). \end{aligned} \quad (3)$$

In the above, m_{l_i} is the projection of l_i .

For the final channel, the wave function is

$$\begin{aligned} \psi_{\vec{k} s_{v_f} m_{v_f} s_{c_f} m_{c_f}}(\vec{r}) = & \sum_{\substack{l_f M_f m'_{l_f} m'_{c_f} \\ l_f m_{l_f} m'_{l_f} \\ L_f M_{L_f} M'_{L_f}}} [(-1)^{l_f + s_{v_f} - M'_{L_f}} \\ & \times \sqrt{2L_f + 1} \begin{pmatrix} l_f & s_{v_f} & L_f \\ m'_{l_f} & m'_{v_f} & -M'_{L_f} \end{pmatrix} Y_{l_f m'_{l_f}}(\hat{r}) \chi_{s_{v_f} m'_{v_f}} \left. \right] \\ & \times (-1)^{L_f + s_{c_f} - M_f} \sqrt{2I_f + 1} \begin{pmatrix} L_f & s_{c_f} & I_f \\ M'_{L_f} & m'_{c_f} & -M_f \end{pmatrix} \\ & \times \chi_{s_{c_f} m'_{c_f}} (-1)^{l_f + s_{v_f} - M_{L_f}} \sqrt{2L_f + 1} \\ & \times \begin{pmatrix} l_f & s_{v_f} & L_f \\ m_{l_f} & m_{v_f} & -M_{L_f} \end{pmatrix} (-1)^{L_f + s_{c_f} - M_f} \sqrt{2I_f + 1} \\ & \times \begin{pmatrix} L_f & s_{c_f} & I_f \\ M_{L_f} & m_{c_f} & -M_f \end{pmatrix} Y_{l_f m_{l_f}}^*(\hat{k}) \frac{1}{r} g_{(L_f s_{c_f}) I_f}(k, r), \end{aligned} \quad (4)$$

where \vec{k} is the wave vector associated with the relative motion between the two fragments in the continuum. l_f is the orbital angular momentum for the core-valence relative motion and I_f is the total spin of the $c + v$ system in the final channel.

We assume that the electromagnetic multipole operators act only on the relative motion variables of the system. This leads to the following conditions: $s_{c_i} = s_{c_f} = s_c$, $s_{v_i} = s_{v_f} = s_v$ and $m_{c_i} = m'_{c_f}$, $m_{v_i} = m'_{v_f}$.

Now we define a reduced matrix element of the multipole operator $M(El, m) (= [Z_c e (\frac{A_v}{A_a})^l +$

$(-1)^l Z_v e (\frac{A_c}{A_a})^l] r^l Y_{lm}(\hat{r}))$ with multipolarity l having projection m) between the final and the initial state:

$$\begin{aligned} & \langle (L_i s_c) I_i || M(El) || (L_f s_c) I_f \rangle = (-1)^{l_i} \\ & \times \sqrt{\frac{(2l_i + 1)(2l_f + 1)(2l + 1)}{4\pi}} \begin{pmatrix} l_i & l & l_f \\ 0 & 0 & 0 \end{pmatrix} \\ & \times [Z_c e (\frac{A_v}{A_a})^l + (-1)^l Z_v e (\frac{A_c}{A_a})^l] \\ & \times \int_0^\infty dr f_{(L_i s_c) I_i}^*(r) \cdot r^l \cdot g_{(L_f s_c) I_f}(k, r). \end{aligned} \quad (5)$$

In Eq.(5), Z_i ($i = c, v$) is the charge of the i th fragment and A_j ($j = c, v, A$) is the mass number of the j th particle.

With this definition, the matrix element of the multipole operator is given by

$$\begin{aligned} & \langle \psi_{I_i M_i} | M(El, m) | \psi_{\vec{k} s_{v_f} m_{v_f} s_{c_f} m_{c_f}} \rangle \\ & = \sum_{\substack{l_i m_{l_i} \\ L_i M_{L_i} \\ m_{v_i} m_{c_i}}} \sum_{\substack{l_f M_f \\ l_f m_{l_f} m'_{l_f} \\ L_f M_{L_f} M'_{L_f}}} (-1)^{-m_{v_i} + L_i + 2L_f + 3s_v + 3s_c - M_i - M_{L_f}} \\ & \times (-1)^{-M'_{L_f} - 2M_f} \sqrt{(2L_i + 1)(2I_i + 1)(2L_f + 1)} \\ & \times (2I_f + 1) \begin{pmatrix} l_i & s_v & L_i \\ m_{l_i} & m_{v_i} & -M_{L_i} \end{pmatrix} \begin{pmatrix} L_i & s_c & I_i \\ M_{L_i} & m_{c_i} & -M_i \end{pmatrix} \\ & \times \begin{pmatrix} l_f & s_v & L_f \\ m'_{l_f} & m_{v_i} & -M'_{L_f} \end{pmatrix} \begin{pmatrix} L_f & s_c & I_f \\ M'_{L_f} & m_{c_i} & -M_f \end{pmatrix} \\ & \times \begin{pmatrix} l_f & s_v & L_f \\ m_{l_f} & m_{v_f} & -M_{L_f} \end{pmatrix} \begin{pmatrix} L_f & s_c & I_f \\ M_{L_f} & m_{c_f} & -M_f \end{pmatrix} \\ & \times \begin{pmatrix} l_i & l & l_f \\ -m_{l_i} & m & m'_{l_f} \end{pmatrix} \langle (L_i s_c) I_i || M(El) || (L_f s_c) I_f \rangle \\ & \times Y_{l_f m_{l_f}}^*(\hat{k}). \end{aligned} \quad (6)$$

The expression for the triple differential cross section for the above electromagnetic breakup process in the incident beam coordinate system (the spins are not observed) is given by

$$\frac{d^3\sigma}{d\Omega_{cv} d\Omega_{cm} dE_{cv}} = \frac{d\sigma^{el}}{d\Omega_{cm}} \rho(E_{cv}) P(\hat{\mathbf{k}}), \quad (7)$$

where $\frac{d\sigma^{el}}{d\Omega_{cm}}$ is the Rutherford scattering cross section and $\rho(E_{cv})$ is the density of final states at relative energy E_{cv} . $P(\hat{\mathbf{k}})$, obtained from the matrix element in Eq.(6) above, is associated with the probability that the two fragments are scattered in the final channel with relative motion wave vector \vec{k} . We expand it in terms of the spherical harmonic $Y_{LM}(\hat{\mathbf{k}})$. It is given by

$$P(\hat{\mathbf{k}}) = \sum_{LM} A_{LM} Y_{LM}(\hat{\mathbf{k}}), \quad (8)$$

where

$$\begin{aligned}
A_{LM} = & \left(\frac{4\pi Z_A e}{\hbar v} \right)^2 \sum_{\substack{l_i m_i' m_i' \\ l_i' L_i' L_f' L_f'}} \sum_{\substack{l_i' l_i' \\ l_f' l_f' \\ l_f' l_f'}} (-1)^{s_c + s_v - l_i - l_i' - L_i - L_i'} \\
& \times (-1)^{-I_f + I_f' - I_i + m} \mathcal{R}^{-(l+l')} \frac{(2I_f + 1)(2I_f' + 1)}{(2l + 1)(2l' + 1)} \\
& \times \sqrt{(2L_i + 1)(2L_i' + 1)(2L_f + 1)(2L_f' + 1)} \\
& \times \sqrt{\frac{(2l_f + 1)(2l_f' + 1)(2L + 1)}{4\pi}} \\
& \times \left[\sum_{nn'} D_{mn}^l \left(-\frac{\pi}{2}, \frac{\pi}{2}, \frac{\pi - \theta_{cm}}{2} \right) D_{m'n'}^{l'\star} \left(-\frac{\pi}{2}, \frac{\pi}{2}, \frac{\pi - \theta_{cm}}{2} \right) \right. \\
& \times Y_{ln} \left(\frac{\pi}{2}, 0 \right) Y_{l'n'} \left(\frac{\pi}{2}, 0 \right) I_{ln}(\theta_{cm}, \xi) I_{l'n'}(\theta_{cm}, \xi) \left. \right] \\
& \times \begin{pmatrix} l_f & l_f' & L \\ 0 & 0 & 0 \end{pmatrix} \begin{pmatrix} l & l' & L \\ m & -m' & -M \end{pmatrix} \begin{Bmatrix} l & l' & L \\ I_f' & I_f & I_i \end{Bmatrix} \\
& \times \begin{Bmatrix} l' & L_i' & L_f' \\ s_v & l_f' & l_i' \end{Bmatrix} \begin{Bmatrix} l & L_i & L_f \\ s_v & l_f & l_i \end{Bmatrix} \begin{Bmatrix} L_f & L_f' & L \\ l_f' & l_f & s_v \end{Bmatrix} \\
& \times \begin{Bmatrix} l & I_i & I_f \\ s_c & L_f & L_i \end{Bmatrix} \begin{Bmatrix} l' & I_i & I_f' \\ s_c & L_f' & L_i' \end{Bmatrix} \begin{Bmatrix} I_f & I_f' & L \\ L_f' & L_f & s_c \end{Bmatrix} \\
& \times \langle (L_i s_c) I_i \parallel M(E_l) \parallel (L_f s_c) I_f \rangle \\
& \times \langle (L_i' s_c) I_i \parallel M(E_{l'}) \parallel (L_f' s_c) I_f' \rangle^*. \tag{9}
\end{aligned}$$

In Eq.(9), \mathcal{R} is half the distance of closest approach in a head-on collision and ξ is the adiabaticity parameter, given as the ratio of the collision time and the excitation time. D_{mn}^l 's are the Wigner D -functions and θ_{cm} is the scattering angle of the c.m. of the projectile. Z_A is the charge number of the target and v is the projectile-target relative velocity in the entrance channel. $I_{ln}(\theta_{cm}, \xi)$ is the classical orbital integral in the focal system of the hyperbolic orbit of the projectile [11].

Through our formalism, we can account for pure dipole ($l = l' = 1$) and pure quadrupole ($l = l' = 2$) transitions as well as mixed transitions ($l = 1, l' = 2$ or $l = 2, l' = 1$) or dipole-quadrupole interference. Also, it is possible to calculate very exclusive observables up to the level of the triple differential cross section. Previous calculations on the breakup of ${}^8\text{B}$ were done by assuming that the angular distribution of fragments is isotropic in the projectile rest frame [12–14]. This approximation gives

$$\frac{d^3\sigma}{d\Omega_{cv} d\Omega_{cm} dE_{cv}} = \frac{1}{4\pi} \frac{d^2\sigma}{d\Omega_{cm} dE_{cv}}. \tag{10}$$

It should be noted that expression for similar triple differential cross section as in Eq.(7) was given by Baur and Weber in Ref. [9], through which it is possible to account for $E1$ and $E2$ contributions separately as well as their interference. However, in contrast to our work, the coupling scheme of angular momenta and spins followed by them does not allow the use of the more detailed coupling scheme adopted here. In fact, the coupling scheme in Ref. [9] is more restricted in the sense that the orbital

angular momentum of the valence particle with respect to the core is coupled to the sum of the spins of c and v both in the initial and the final channel.

We note that integration over the solid angle associated with the relative motion of the fragments gives

$$\frac{d^2\sigma}{d\Omega_{cm} dE_{cv}} = \sqrt{4\pi} \frac{d\sigma^{el}}{d\Omega_{cm}} \rho(E_{cv}) A_{00}, \tag{11}$$

which is free from the $E1 - E2$ interference term, since A_{00} (with $L, M = 0$) does not involve these terms. This is evident from the 3-j symbol $\begin{pmatrix} l & l' & L \\ m & -m' & -M \end{pmatrix}$ occurring in Eq.(9), because for $L = 0$, l and l' must be the same. Thus, any cross section obtained from the above triple differential cross section (Eq.(7)) by integration with respect to the solid angle Ω_{cv} is free from $E1 - E2$ interference. This result is independent of the structure models of ${}^8\text{B}$. Therefore, the analyses presented in Refs. [7,8,13,14] are indeed free from the $E1 - E2$ interference effects.

III. STRUCTURE MODEL

The calculations of the reduced matrix elements involved in Eq.(9) require the detailed knowledge of ground state as well as continuum structure of ${}^8\text{B}$, which is not yet known with certainty. In our calculations, we adopt the single particle potential model (SPPM) for ${}^8\text{B}$ [3]. It is to be noted that the matrix elements of the multipole operators enter directly into these calculations. Therefore, they are quite sensitive to the structure model of ${}^8\text{B}$.

Within the SPPM, the valence proton (with spin $\frac{1}{2}$) in ${}^8\text{B}$ (with spin-parity 2^+) is assumed to move relative to an inert ${}^7\text{Be}$ core (with intrinsic spin-parity $3/2^-$) in a Coulomb field and a Woods-Saxon plus spin-orbit potential, with an adjustable depth $V_0(l(Ls_c)I)$ for the initial and each final channel:

$$V(r) = V_0(l(Ls_c)I) \left(1 - F_{s.o.}(\vec{l}, \vec{s}) \frac{r_0}{r} \frac{d}{dr} \right) f(r), \tag{12}$$

where

$$f(r) = (1 + \exp((r - R)/a))^{-1}. \tag{13}$$

Adjusting the depth allows one to reproduce the energy of the known states. We use $a=0.52$ fm, $r_0=1.25$ fm and $R=2.391$ fm [3]. The spin-orbit strength is set to $F_{s.o.} = 0.351$ fm [3]. The rms distance of the core-proton relative motion and the rms size of ${}^8\text{B}$ come out to be 4.24 fm and 2.64 fm respectively.

The well depth for the ground state channel, $V_0(l_i(L_i s_c)I_i) = V_0((p_{3/2}, 3/2^-)2^+)$, was adjusted to reproduce the one-proton separation energy of 0.137 MeV. It came out to be -44.658 MeV). Similarly, the observed $I_f = 1^+$ and 3^+ resonances in ${}^8\text{B}$ are described as $p_{3/2}$

waves coupled to the ground state of the core, and the well depths for these channels, -42.14 and -36.80 MeV, respectively, have been adjusted to reproduce the known resonance energies (0.637 and 2.183 MeV respectively) [15]. A $p_{3/2}$ wave and the spin of the core can also couple to the total spin 0^+ . But we ignore this channel since it appears to be very weak in the low-lying excitation spectrum of ${}^8\text{B}$. For all other partial waves ($s_{1/2}, p_{1/2}, d_{3/2}$ etc.) we choose identical well depths and set them equal to the value -42.14 MeV obtained for the $(p_{3/2}, 3/2^-)1^+$ channel, as suggested by Robertson [16].

IV. RESULTS AND DISCUSSIONS

To check the accuracy of our formulation, we present in Fig. 1 a comparison of our calculations with the data [17] for the triple differential cross sections for the reaction ${}^6\text{Li} + \text{Pb} \rightarrow \alpha + d + \text{Pb}$ at 156 MeV beam energy as a function of the relative energy between the alpha particle and the deuteron for $\theta_\alpha = \theta_d = 3^\circ$. Only $E2$ excitation contributes in this case. Since the multipole charge for the dipole case is zero for ${}^6\text{Li}$ (Eq.(5)), the $E1$ contribution is zero. We have assumed ${}^6\text{Li}$ to be a cluster of α particle and deuteron, for which the structure model

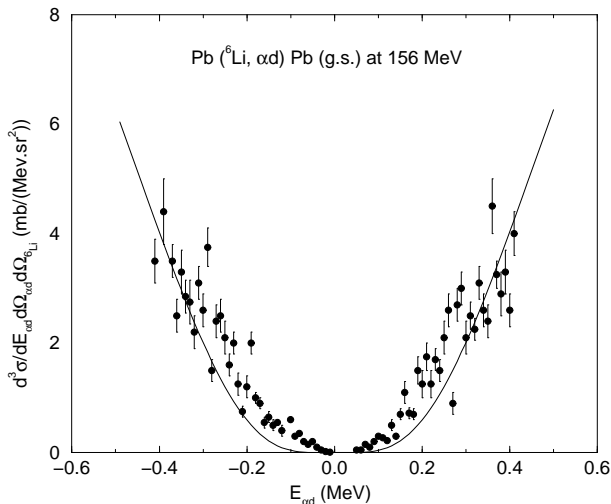


FIG. 1. Triple differential cross section $\frac{d^3\sigma}{d\Omega_\alpha d\Omega_d dE_{\alpha d}}$ for Coulomb breakup of ${}^6\text{Li}$ on Pb at 156 MeV beam energy as a function of $E_{\alpha d}$ for $\theta_{6\text{Li}} = 3^\circ$ and $\theta_{\alpha d} = 0^\circ$. The data have been taken from [17]. Positive $E_{\alpha d}$ implies velocity of α particle is larger than that of deuteron, while negative $E_{\alpha d}$ corresponds to larger deuteron velocity than that of α particle.

of Ref. [18] has been used. We note that our calculations are in good agreement with the data. It may be noted that for the results presented in Ref. [9] for the same reaction, the structure part has been obtained from a constant astrophysical S -factor of 1.7×10^{-5} MeV.mb, and not by using proper wave functions for the ground state and excited states of ${}^6\text{Li}$ as has been done by us. In these

data the contributions from nuclear excitation effects are negligible as the fragments have been detected at very forward angles [19].

In Fig. 2, we present the results of our calculations for the triple differential cross section (Eq.(7)) for Coulomb breakup of ${}^8\text{B}$ on a Pb target at 46.5 MeV/nucleon beam energy as a function of θ_{cm} for relative energy $E_{cv} = 0.2$ MeV and $\theta_{cv} = 1^\circ$ (top half) and as a function of E_{cv} for $\theta_{cm} = 3^\circ$ and $\theta_{cv} = 1^\circ$ (bottom half). We see that the $E1 - E2$ interference (long dashed line) contribution is quite important in both cases. In fact, it is larger than the $E2$ contribution (dashed line) and modifies the coherent sum (solid line) of $E1$ (dotted line) and $E2$ cross sections significantly. It may be noted that this type of triple differential cross sections have not yet been measured for reactions involving unstable radioactive nuclei (e.g. ${}^8\text{B}$).

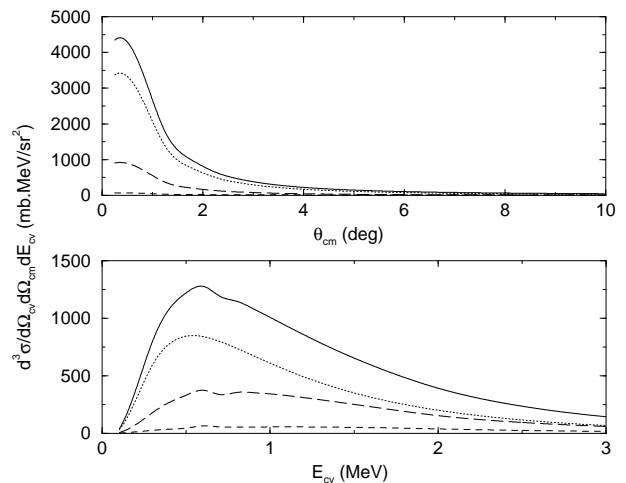


FIG. 2. $E1$ (dotted line), $E2$ (dashed line) components together with the $E1 - E2$ interference (long dashed line) contribution in the triple differential cross section $\frac{d^3\sigma}{d\Omega_{cv} d\Omega_{cm} dE_{cv}}$ for Coulomb breakup of ${}^8\text{B}$ on Pb at 46.5 MeV/nucleon beam energy as a function of θ_{cm} for $E_{cv} = 0.2$ MeV and $\theta_{cv} = 1^\circ$ (top half) and as a function of E_{cv} for $\theta_{cm} = 3^\circ$ and $\theta_{cv} = 1^\circ$ (bottom half). The solid line in each case shows the coherent sum of $E1$ and $E2$ cross sections.

However, the differential cross section $\frac{d\sigma}{d\theta_{cm}}$ has been measured as a function of θ_{cm} in the dissociation of ${}^8\text{B}$ on Pb at beam energies ~ 50 MeV/nucleon at RIKEN [7,8]. At larger scattering angles the cross sections are more sensitive to the $E2$ component. A detailed investigation of this reaction was carried out in Ref. [13] by assuming the fragment emission to be isotropic in the projectile rest frame (Eq.(10)).

In Fig. 3, we present our calculations for the different components in the Coulomb breakup cross section for this reaction at the beam energy of 51.9 MeV/nucleon, by using our formalism (i.e. without making the approximation of isotropic emission). For this observable the coherent sum (solid line) of $E1$ (dotted line) and $E2$

(dashed line) contributions is simply the sum of these two separate cross sections, as there is no contribution from the $E1 - E2$ interference component as discussed above (see Eq.(11)). We note that the results presented in Fig. 3 are the same as the pure Coulomb dissociation (with semiclassical theory) results presented in Ref. [20], which have been obtained with the isotropic emission assumption. These calculations, however, use a different structure model for ${}^8\text{B}$, namely, the shell model embedded in the continuum. Therefore, the present calculations give credence to the calculations reported in Ref. [20]. As discussed earlier in Refs. [13,20], the disagreement between the data and the calculations beyond 4° in this figure can be attributed to the point like projectile approximation of the semiclassical theory, which is no longer valid for larger angles. Inclusion of finite size effects in the calculations leads to better agreement between data and the theoretical results [13]. It should also be mentioned that the nuclear breakup effects are important only at larger angles ($> 4^\circ$) in all the three energy bins [13,21].

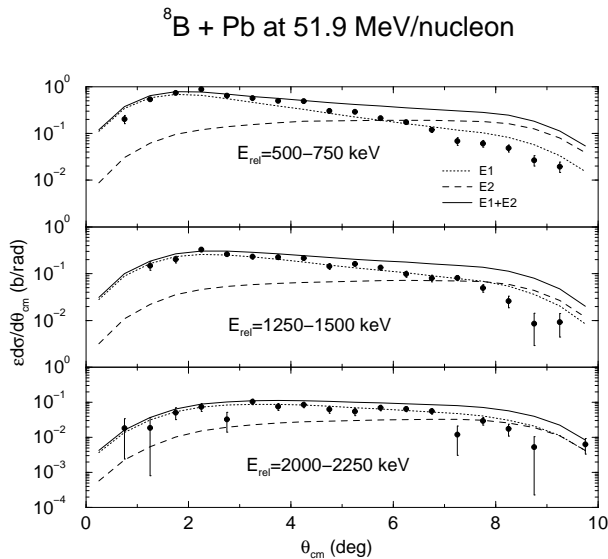


FIG. 3. Calculated differential cross section $\epsilon \frac{d\sigma}{d\theta_{cm}}$ for Coulomb breakup of ${}^8\text{B}$ on Pb at 51.9 MeV/nucleon for three given relative energy bins as a function of θ_{cm} . The cross sections have been folded with experimental efficiency. The data, which are also folded with experimental efficiency, have been taken from [8].

The triple differential cross section $\frac{d^3\sigma}{d\Omega_{cv}d\Omega_{cm}dE_{cv}}$ can be related to that of the individual fragments c and v ($\frac{d^3\sigma}{dE_c d\Omega_c d\Omega_v}$) [22]. Since interference contributions are significant in $\frac{d^3\sigma}{d\Omega_{cv}d\Omega_{cm}dE_{cv}}$, it is expected that they would also be important in $\frac{d^3\sigma}{dE_c d\Omega_c d\Omega_v}$ in general. This is, indeed, the case as can be seen in Fig. 4. In this figure, we have plotted $\frac{d^3\sigma}{dE_c d\Omega_c d\Omega_v}$ (with $c \equiv {}^7\text{Be}$ and $v \equiv p$) as a function of $\theta_{7\text{Be}}$ for Coulomb breakup of ${}^8\text{B}$ on ${}^{58}\text{Ni}$ at the beam energy of 25.8 MeV, for $E_{7\text{Be}} = 22.575$ MeV

(the beam velocity energy), $\theta_p = 20^\circ$ and $\phi_p = 0^\circ$. We see that the $E1 - E2$ interference term is quite significant and is even larger than that of the dipole component.

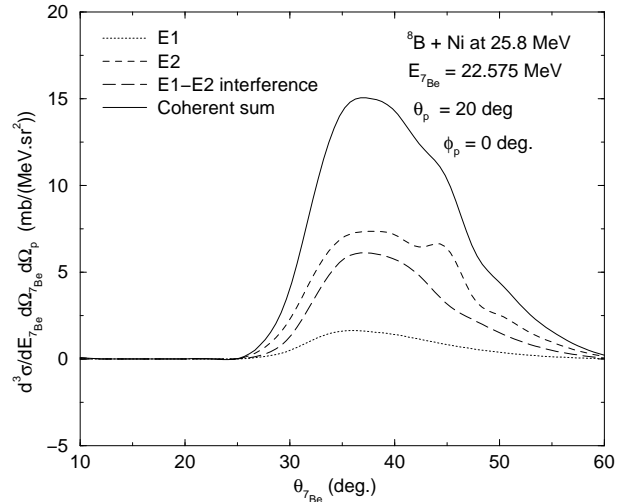


FIG. 4. $E1$ (dotted line), $E2$ (dashed line) components together with the $E1 - E2$ interference (long dashed line) contribution in the triple differential cross section $\frac{d^3\sigma}{dE_{7\text{Be}}d\Omega_{7\text{Be}}d\Omega_p}$ for Coulomb breakup of ${}^8\text{B}$ on Ni at 25.8 MeV beam energy as a function of $\theta_{7\text{Be}}$ for $E_{7\text{Be}} = 22.575$ MeV, $\theta_p = 20^\circ$ and $\phi_p = 0^\circ$. The solid line shows the coherent sum of $E1$ and $E2$ cross sections.

However, for less exclusive observables (like the angular distribution of individual fragments) the interference term is not so strong. This can be seen in Fig. 5, where we show the ${}^7\text{Be}$ angular distribution resulting from the Coulomb dissociation of ${}^8\text{B}$ on a Ni target at 25.8 MeV. We note that the $E1 - E2$ interference (long dashed line) is small in magnitude compared to the dipole (dotted line) and quadrupole (dashed line) breakup cross sections, excepting at larger angles (around 75°) where it is comparable in magnitude to the $E1$ component. The interference component oscillates between positive and negative values which is also reflected in the coherent sum of the $E1$ and $E2$ cross sections (solid line).

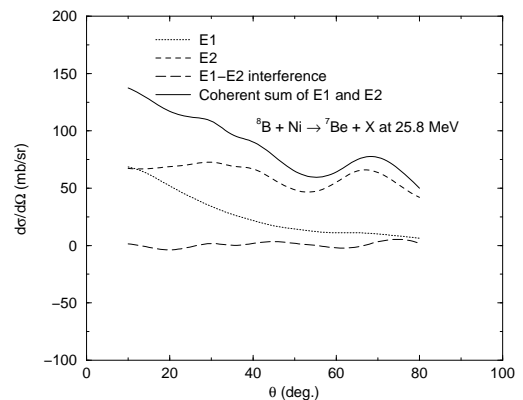


FIG. 5. $E1$ (dotted line), $E2$ (dashed line) components together with the $E1-E2$ interference (long dashed line) contribution in the ${}^7\text{Be}$ angular distribution for Coulomb breakup of ${}^8\text{B}$ on Ni at 25.8 MeV beam energy. The solid line shows the coherent sum of $E1$ and $E2$ cross sections.

To understand why the interference is not large in the ${}^7\text{Be}$ angular distribution shown in Fig. 5, we have plotted in Fig. 6 the θ_p (top half, with typical value of $\phi_p = 10^\circ$) and ϕ_p (bottom half, with typical value of $\theta_p = 20^\circ$) variations of the interference term in the triple differential cross section shown in Fig. 4 for typical energy and angle of the ${}^7\text{Be}$ fragment $E_{7\text{Be}} = 22.575$ MeV and $\theta_{7\text{Be}} = 10^\circ$ respectively. The variation patterns are oscillatory and show positive and negative values of almost equal magnitudes. For some angles the cross sections are very small. Therefore, it is no surprise that integrations with respect to the polar and azimuthal angles of the proton will lead to cancellation and hence to small magnitudes of the interference term in the overall ${}^7\text{Be}$ angular distribution.

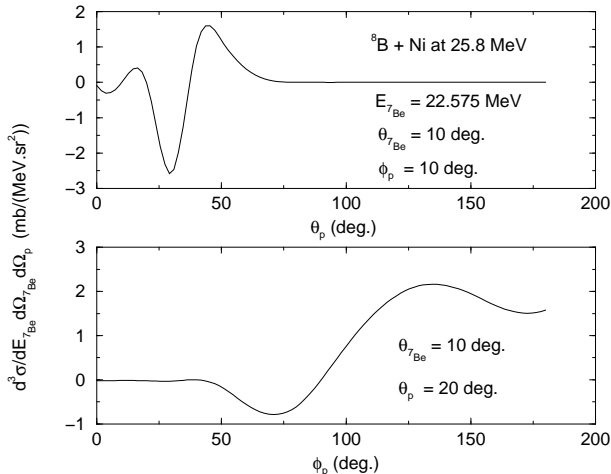


FIG. 6. θ_p (top half, $\phi_p = 10^\circ$) and ϕ_p (bottom half, $\theta_p = 20^\circ$) variations in the $E1-E2$ interference contribution in the triple differential cross section $\frac{d^3\sigma}{dE_{7\text{Be}}d\Omega_{7\text{Be}}d\Omega_p}$ for Coulomb breakup of ${}^8\text{B}$ on Ni at 25.8 MeV beam energy for $E_{7\text{Be}} = 22.575$ MeV and $\theta_{7\text{Be}} = 10^\circ$.

However, there is still a remaining question of the effects of strong (nuclear) interaction between the colliding nuclei. They can be almost eliminated by choosing the proper kinematical conditions. For example, the ${}^8\text{B}$ breakup data taken by the RIKEN collaboration [7,8] have been shown [13,21,23] to be almost free from the nuclear effects for ${}^7\text{Be}-p$ relative energies ≤ 0.75 MeV at very forward angles ($\leq 4^\circ$). Similarly the data taken at GSI [24] at higher beam energy of ~ 250 MeV/A are also free from these effects (see *e.g.* [25]). Therefore, the results presented in Fig. 2 are unlikely to be affected by nuclear excitation. However, these effects can be quite strong [13] for the breakup studies [6,26] at lower

beam energies (~ 25 MeV). In any case, it is straightforward to calculate [27] the amplitudes for pure nuclear and Coulomb-nuclear interference terms for the dipole and quadrupole excitations as well as of their interference.

V. SUMMARY AND CONCLUSIONS

In summary, we have performed first order semiclassical calculations of the electromagnetic excitation of ${}^8\text{B}$, where the electric dipole and quadrupole excitation components as well as their interference effects are included. The theory permits consideration of coupling of angular momenta and spins of the projectile fragments in detail. It is possible to calculate exclusive observables to the level of the triple differential cross section within this formalism.

We find that the magnitude of the $E1-E2$ interference term could be appreciable in the triple differential cross sections. However, observables which are not functions of the solid angle associated with the relative motion of the breakup fragments in the final channel, are free from this term. This result is independent of the structure models of ${}^8\text{B}$. We have also shown that for double differential cross sections involving angle of scattering of the projectile with respect to the target and energy of relative motion between the projectile fragments, the approximation of the isotropic emission in the rest frame of the projectile is quite good. Therefore, analysis of the RIKEN data presented earlier using this approximation is quite accurate and this data, in the proper kinematical regime ($\theta_{sB^*} < 4^\circ$ and $E_{7\text{Be}-p} \leq 500$ keV) can be used to extract rather reliable astrophysical S -factor $S_{17}(0)$.

The interference terms are also significant in the triple differential cross sections of the individual fragments. However, in the angular distribution of the individual fragments these terms are not significant. Therefore, the experimental data present in Ref. [26] are almost free from the $E1-E2$ interference terms. However, the effects of the three body kinematics (not considered in the analysis of these data) may still be important.

-
- [1] G. Baur and H. Rebel, J. Phys. G **20**, 1 (1994); Ann. Rev. Nucl. Part. Sc. **46**, 321 (1997).
 - [2] J. N. Bahcall, *Neutrino Astrophysics*, Cambridge University Press, New York, 1989; J. N. Bahcall and M. H. Pinsonneault, Rev. Mod. Phys. **67**, 781 (1995); J. N. Bahcall, Nucl. Phys. **A631**, 29 (1998).
 - [3] H. Esbensen and G. F. Bertsch, Phys. Lett. **B359**, 13 (1995); Nucl. Phys. **A600**, 37 (1996).
 - [4] C. A. Bertulani, Z. Phys. A **356**, 293 (1996).
 - [5] B. Davids *et al.*, Phys. Rev. Lett. **81**, 2209 (1998).

- [6] J. von Schwarzenberg *et al.*, Phys. Rev. C **53**, R2598 (1996).
- [7] T. Motobayashi *et al.*, Phys. Rev. Lett. **73**, 2680 (1994).
- [8] T. Kikuchi *et al.*, Phys. Lett. B **391**, 261 (1997); T. Kikuchi *et al.*, Eur. Phys. J. A **3**, 213 (1998).
- [9] G. Baur and M. Weber, Nucl. Phys. A **504**, 352 (1989).
- [10] R. Shyam and I. J. Thompson, *PRAMANA – J.Phys.* **53**, 595 (1999).
- [11] K. Alder and A. Winther, *Electromagnetic Excitation* (North Holland, Amsterdam, 1975).
- [12] C. A. Bertulani, Phys. Rev. C **49**, 2688 (1994).
- [13] R. Shyam and I. J. Thompson, Phys. Rev. C **59**, 2645 (1999).
- [14] R. Shyam and I. J. Thompson, Phys. Lett. B **415**, 315 (1997).
- [15] F. Ajzenberg-Selove, Nucl. Phys. A **490**, 103 (1988).
- [16] R. G. H. Robertson, Phys. Rev. C **7**, 543 (1973).
- [17] J. Kiener, H. J. Gils, H. Rebel and G. Baur, Z. Phys. A **332**, 359 (1989).
- [18] H. Nishioka, J. A. Tostevin, R. C. Johnson and K.-I. Kubo, Nucl. Phys. A **415**, 230 (1984).
- [19] R. Shyam, G. Baur and P. Banerjee, Phys. Rev. C **44**, 915 (1991).
- [20] R. Shyam, K. Bennaceur, J. Okolowicz and M. Ploszajczak, Nucl. Phys. A **669**, 65 (2000).
- [21] C.A. Bertulani and M. Gai, Nucl. Phys. A **636**, 227 (1998).
- [22] F. Fuchs, Nucl. Instr. & Methods, **200**, 361 (1982).
- [23] R. Shyam, I.J. Thompson and A.K. Dutt-Majumder, Phys. Lett. B **371**, 1 (1996).
- [24] N. Iwasa *et al.*, Phys. Rev. Lett. **83**, 2910 (1999).
- [25] G. Baur, K. Henken, D. Trautmann, S. Typel and W. Wolter, LANL preprint nucl-th/0008033.
- [26] V. Guimarães *et al.*, Phys. Rev. Lett. **84**, 1862 (2000).
- [27] F. Rybicki and N. Austern, Phys. Rev. C **6**, 1525 (1971).